Supporting Information

Coordinative interaction between nitrogen oxides and iron-molybdenum POM $Mo_{72}Fe_{30}$

Kirill V. Grzhegorzhevskii,*[a] Margarita O. Tonkushina,[a] Andrei V. Fokin,[a] Ksenia G. Belova[a, b] and Alexander A. Ostroushko[a]

[a] *Institute of Natural Sciences and Mathematics, Ural Federal University named after the B.N. Yeltsin, 620002, Ekaterinburg, Russia*

[b] *Institute of High Temperature Electrochemistry, 620137, Ekaterinburg, Russia*

Calculation of water molecules content in the POM-NO_2 sample

Calculation of water molecules content in the POM-NO_2 sample was performed using the data of elemental analysis, which showed the reduction of hydrogen's weight-part from 2.84 (for $Mo_{72}Fe_{30}$) to 1.65 w.% (for POM-NO_2). As it was mentioned in article, the composition of $Mo_{72}Fe_{30}$ is represented by formula: $[Mo_{72}Fe_{30}O_{252}(CH_3COO)_{12}\{Mo_2O_7(H_2O)\}_2\{H_2Mo_2O_8(H_2O)\}(H_2O)_{91}]\cdot 150H_2O$. Totally, there are 226 hydrogen atoms excluding non-constitutional 150 water molecules. For our calculation, we used the simple system with three unknowns:

$$x = 226 + y$$

$$w = \frac{x \times M_H}{M_S + z}$$

$$z = \frac{y}{2} \times M_W$$

where: x – number of hydrogen atoms including non-constitutional water molecules of POM-NO_2; y – number of hydrogen atoms from non-constitutional water molecules; z – mass of all non-constitutional water molecules; M_H – atomic weight of hydrogen; M_W – molecular mass of H_2O; M_S – molar mass of sample (POM-NO_2) without non-constitutional water molecules, which was established as molar mass of $Mo_{72}Fe_{30}$ (18648.85 g/mol) minus molar mass of 150 water molecules and plus molar mass of six stoichiometric NO_2 molecules.

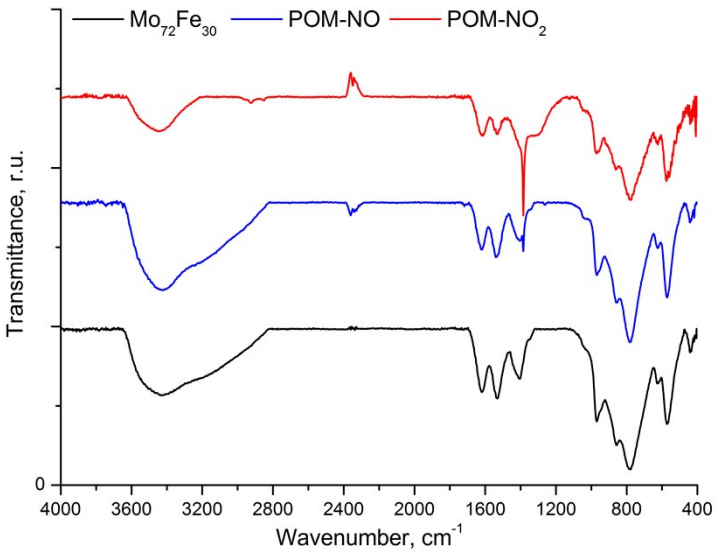

Fig. S1. Full-range IR spectra of solid samples $Mo_{72}Fe_{30}$, POM-NO, POM-NO_2 in dry KBr pellets on air atmosphere.

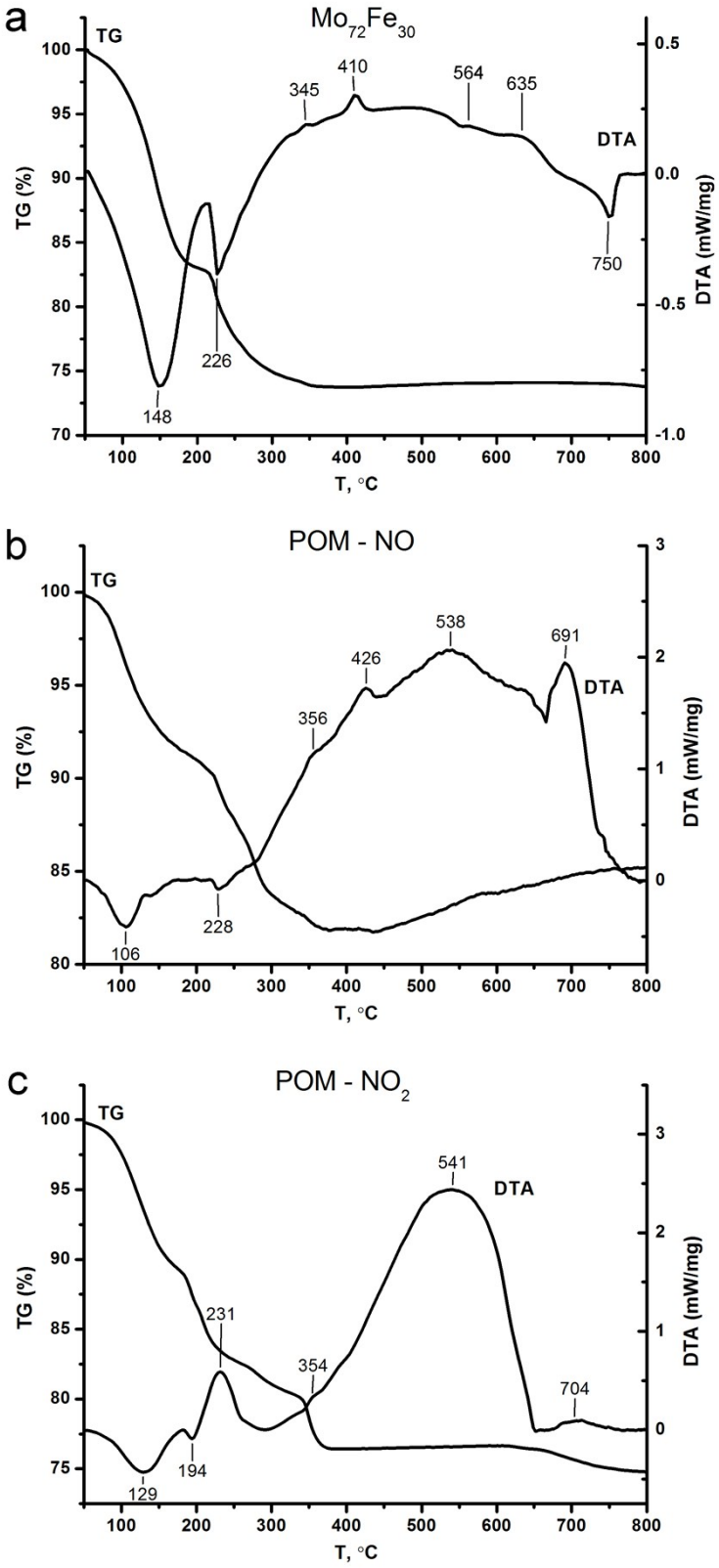

Fig. S2. TG-DTA analysis of (a) – $Mo_{72}Fe_{30}$, (b) – POM-NO, (c) – POM-NO_2.

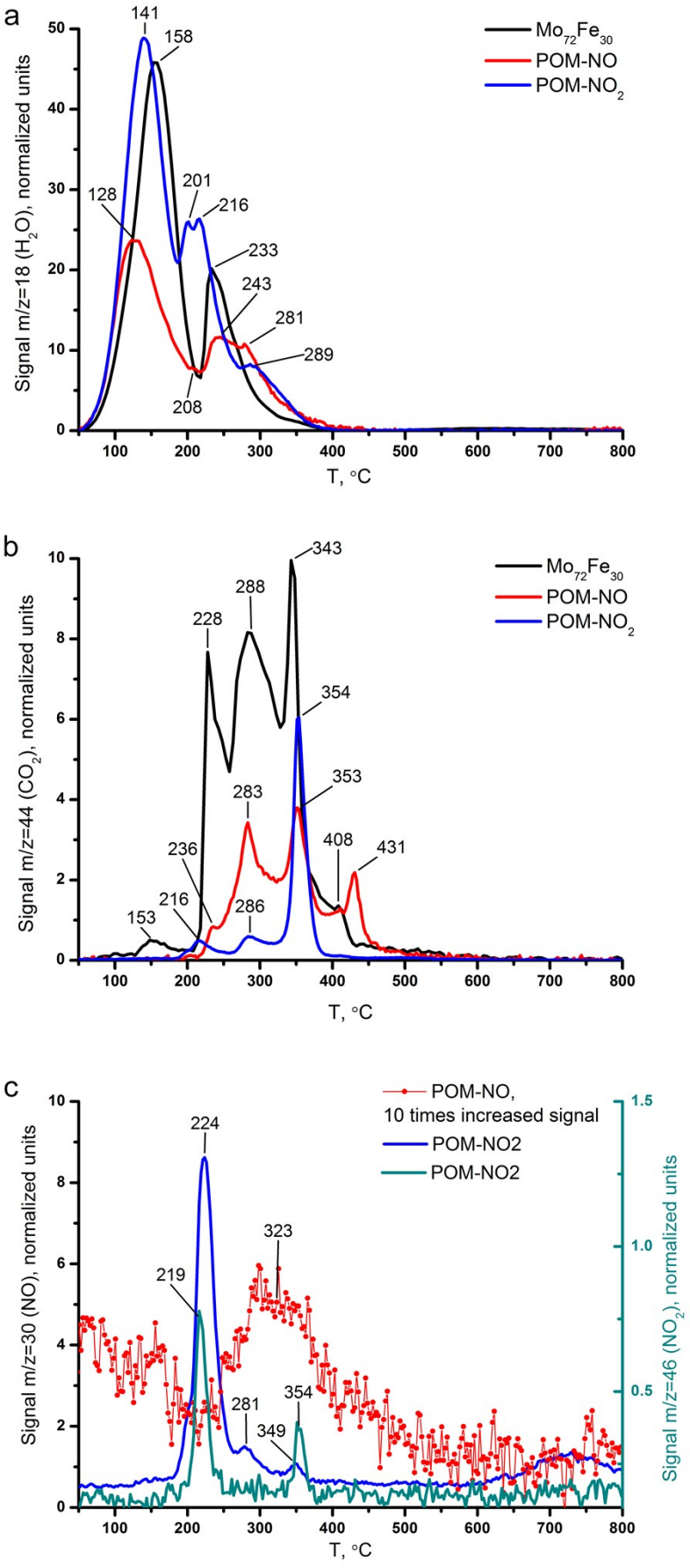

Fig. S3. Mass-spectral analysis of $Mo_{72}Fe_{30}$, POM-NO, POM-NO_2 samples for m/q 18 - H_2O (a), 44 - CO_2 (b), 30 and 46 – NO and NO_2 (c).

TGA/DTA studies coupled with mass-spectrometry analysis of gaseous phase

In order to clarify some implicit points in the interpretation of thermal destruction process for samples studied, we put the detailed explanation into the supporting information and presented in a list:

1. In context of water releasing, we should pay an attention to common weight loss of samples (Table 1, see manuscript). As one may see, the $Mo_{72}Fe_{30}$ and POM-NO_2 possess a similar value of this parameter: -28.34 and -25.22%, respectively, whereas the final weigh loss for POM-NO sample is -14.80%. The reason of this difference is due to the synthesis condition of POM-NO sample, which was produced by the treatment of $Mo_{72}Fe_{30}$ with NO gas in the flow of argon during the 30 min. The latter results in the removing of some amount of weakly-bonded water from $Mo_{72}Fe_{30}$ crystal and, consequently, to reducing the final weight loss of POM-NO and its molecular mass. This explanation is confirmed by the smaller weight loss of POM-NO at the initial stages (up to 215 °C), as compared with other samples, caused with the water releasing: -9.2% for POM-NO against the -17.4 and 16.27 % for $Mo_{72}Fe_{30}$ and POM-NO_2, respectively. Moreover, the gradual rise of weight at the high temperature region, observed for all samples, achieves the larger value for POM-NO, in particular. This process is conditioned with the absorption of residual oxygen from the gaseous phase by solid DP and, in accordance with lesser initial molecular weight of POM-NO as compared with $Mo_{72}Fe_{30}$, it leads to relatively higher increasing of sample weigh in percentage scale at the final stage.

2. Under 100 eV electron-beam ionization the NO^+:NO_2^+ ratio of ions' currents strongly depends on the coexisting ions, thus at the presence of CO^+, CO_2^+, O^+ and Ar^+ (the major component of gaseous mixture analyzed) the ion current of m/q=30 has to be several times greater than that for m/q=46 signal[1].

3. Interestingly, the first peak of NO releasing observed at 231 °C is perfectly matched with first peak of m/q=46 signal, whereas among the other m/q=30 signals, revealing at the higher temperature, only peak near 350 °C corresponds to the m/q=46 signal again (Fig. S3). The observed m/q=30 signal at 350 °C has a considerably less intensity than expected from the comparison with related m/q=46 peak, which intensity should be complied to the certain NO^+:NO_2^+ ratio[1]. Thus, we may conclude that observed m/q=46 signal at 350 °C does not refer to the NO_2 evolving from POM-NO_2. Taking into account the active process of acetic acid residues decomposition under this temperature, the foresaid m/q=46 peak can be assigned with one of the possible destruction products of acetate groups, i.e. $HCOOH^+$.

4. Discussing the observation of m/q=44 signal we should take account for the possible alternative particles with this m/q value in addition to CO_2. In the case of POM-NO_2, the emitted NO_2^+ particles can be involved in the additional reaction at

the corresponding temperature. As well-known[2–4], iron cations (belonging to oxides) can play the role of catalytic centres for joint conversion of CO to CO_2 and of NO_2/NO to N_2 or N_2O under inert atmosphere (in particular, reduction atmosphere). In the case of Fe_2O_3, this process occurs stepwise through the formation of partially reduced Fe_2O_2 cluster and CO_2 (m/q=44) molecules, then after NO_x adsorption via multiple oxidation and reduction steps, the oxidized state Fe_2O_3 is returned and N_2O molecule (m/q=44) is produced[2]. In the current study, for all samples, the presence of CO molecules is observed in the small amount (m/q=28) as a result of acetic acid residues thermal destruction[5]. During the destruction process, the CO molecules might be primarily attached to the surface of nanocluster's DP. Thus, it excludes the additional stage of their adsorption from the gaseous phase and facilitates the catalytic conversion of carbon monoxide to CO_2 accompanied with NO_x reduction to N_2O, in particular. On the mass spectra, the signal of CO (m/q=28) is well registered at 350 °C but possesses a small intensity, that is explained with its fast conversion to the CO_2. In the frame of carried experiment the separation of N_2O and CO_2 signals, having the same m/q value, is impossible, but the existence of N_2O particles in the gaseous phase could not be neglected.

5. The nature of the observed exothermic effects for POM-NO_2 accompanied NO_2 releasing at 231 °C (Fig. S2c) and CO_2 evolving near 350 and 420 °C (Fig. S2a,b) should be commented additionally. The carbon dioxide can be produced by the two exothermic reactions. First of them, which was described above, is catalytic conversion of CO by NO_x reduction. The second process is an oxidation of CH_3COO^- groups on the catalytic surface of nanocluster's DP by the residual oxygen (0.004%) of the gaseous phase or by the constitutional oxygen of DP leading to the reduction of the latter ones (standard ΔH of CO combustion is -876.1 kJ/mol, as calculated with data of standard enthalpy of formation[6]). In the case of NO_2 releasing, the exothermic peak is also conditioned by the abovementioned catalytic conversion of CO to the CO_2. The heat evolution, accompanied this conversion, is sufficient to overcome the endothermic effect corresponding to desorption of nitrogen dioxide at the 231 °C (Fig. S2c).

Table S1 XPS signals of $Mo_{72}Fe_{30}$ and POM-NO_2

#	Signal	BE, eV	FWHM, eV	Area, arb. un.
		$Mo_{72}Fe_{30}$		
1	Mo, $3d_{5/2}$	232.95	1.1	212502
	Mo, $3d_{3/2}$	236.11	1.1	138036
2	Fe, $2p_{3/2}$	709.31	1.05	5856
	Fe, $2p_{1/2}$	722.88	1.05	3031
3	Fe, $2p_{3/2}$	711.6	3.5	55133
	Fe, $2p_{1/2}$	724.87	3.5	28536
4	Fe, $2p_{3/2}$	715.49	3.5	20788
	Fe, $2p_{1/2}$	728.29	3.5	10759
5	Fe, $2p_{3/2}$	719.98	3.5	10186
	Fe, $2p_{1/2}$	733.38	3.5	5823
6	Mo, $3p_{3/2}$	398.78	2.7	168982
		POM-NO_2		
1	Mo, $3d_{5/2}$	232.7	1.22	43749
	Mo, $3d_{3/2}$	235.75	1.22	30204
2	Mo, $3d_{5/2}$	233.38	1.68	44434
	Mo, $3d_{3/2}$	236.54	1.68	30472
3	Fe, $2p_{3/2}$	711.89	3.29	18622
	Fe, $2p_{1/2}$	725.31	3.29	9638
4	Fe, $2p_{3/2}$	715.19	3.51	12716
	Fe, $2p_{1/2}$	728.39	3.51	6526
5	Fe, $2p_{3/2}$	720.48	3.52	7950
	Fe, $2p_{1/2}$	733.88	3.52	2245
6	Mo, $3p_{3/2}$	398.78	3.08	66685
7	N, $1s_{1/2}$	406.76	1.41	1762

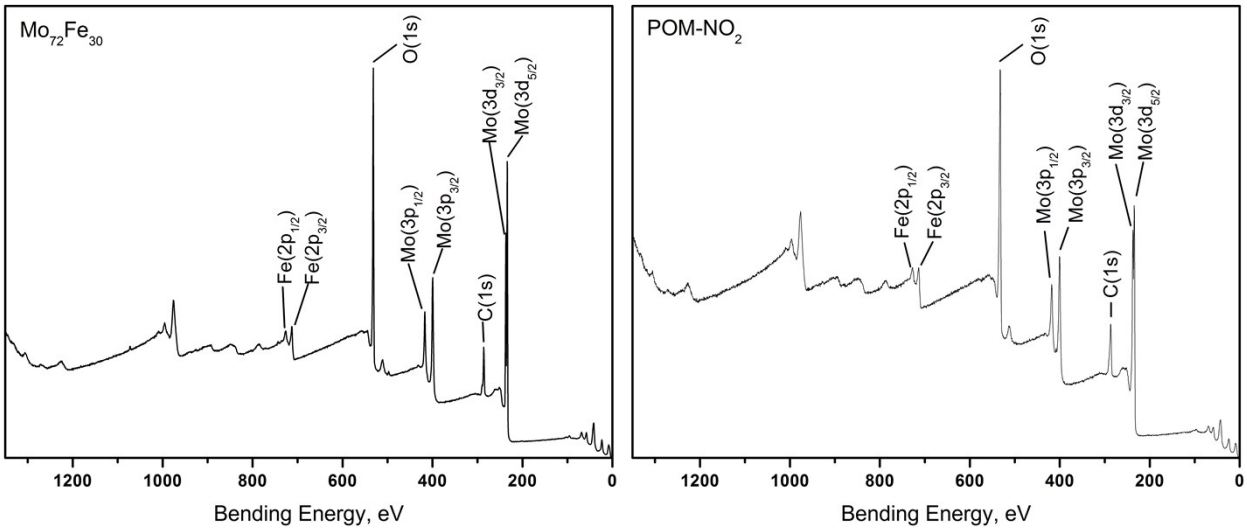

Fig. S4. Survey XPS spectra of the $Mo_{72}Fe_{30}$ and POM-NO_2 samples.

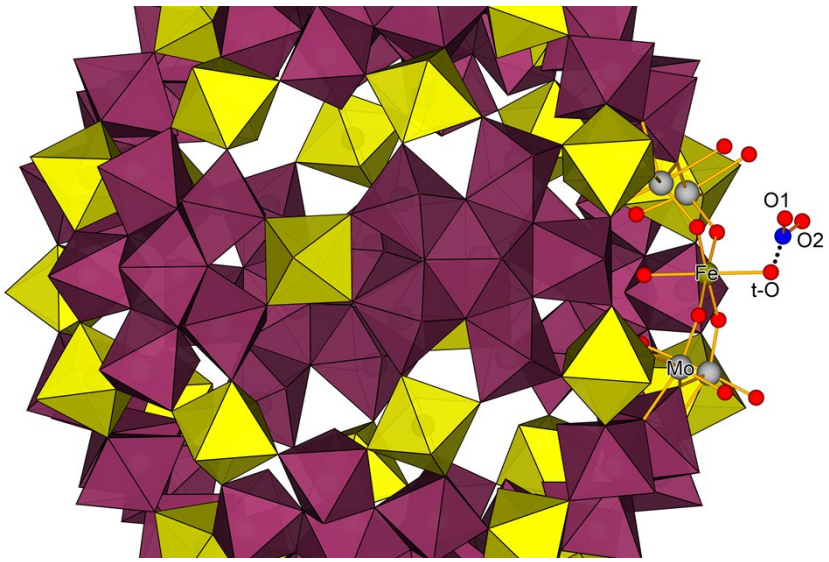

Fig. S5. The model of NO_2 (nitrogen is blue atom) coordination to the terminal oxygen (t-O) in bond Mo-O-Fe outside the SP ("out-of-plane coordination").

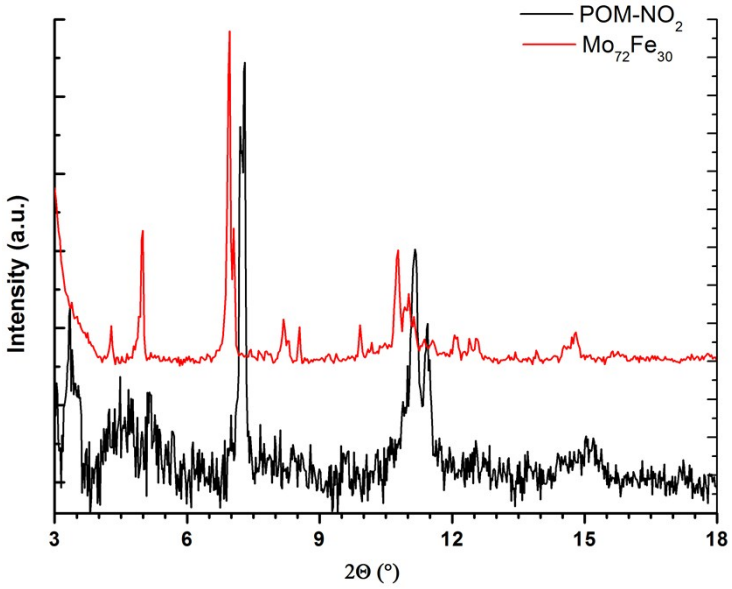

Fig. S6. Diffractogram of $Mo_{72}Fe_{30}$ and POM-NO_2 samples under ambient condition.

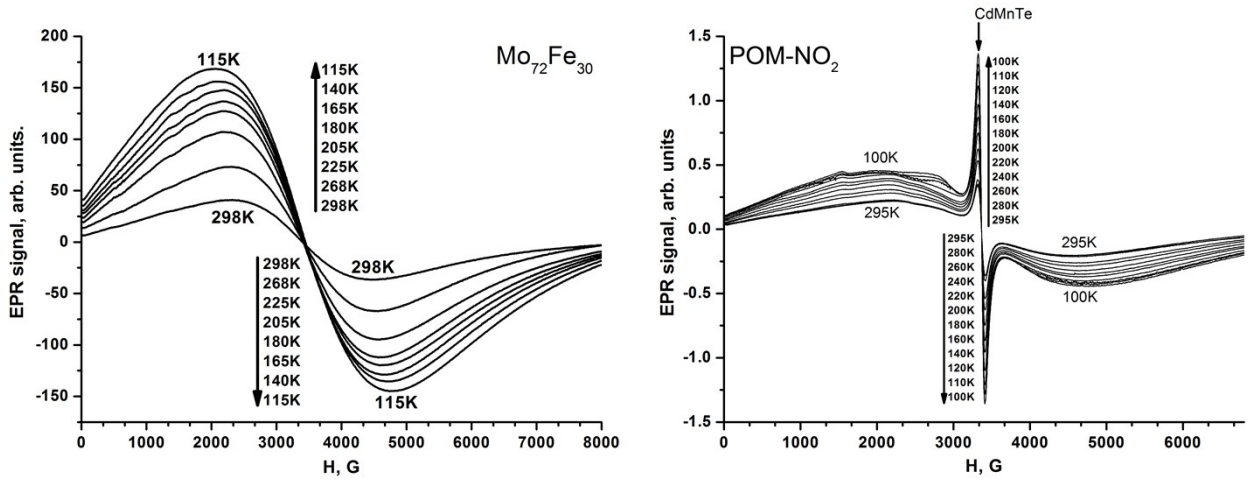

Fig. S7. The temperature dependence of the survey EPR spectra (derivative of the adsorption signal) for $Mo_{72}Fe_{30}$ and POM-NO_2 sample.

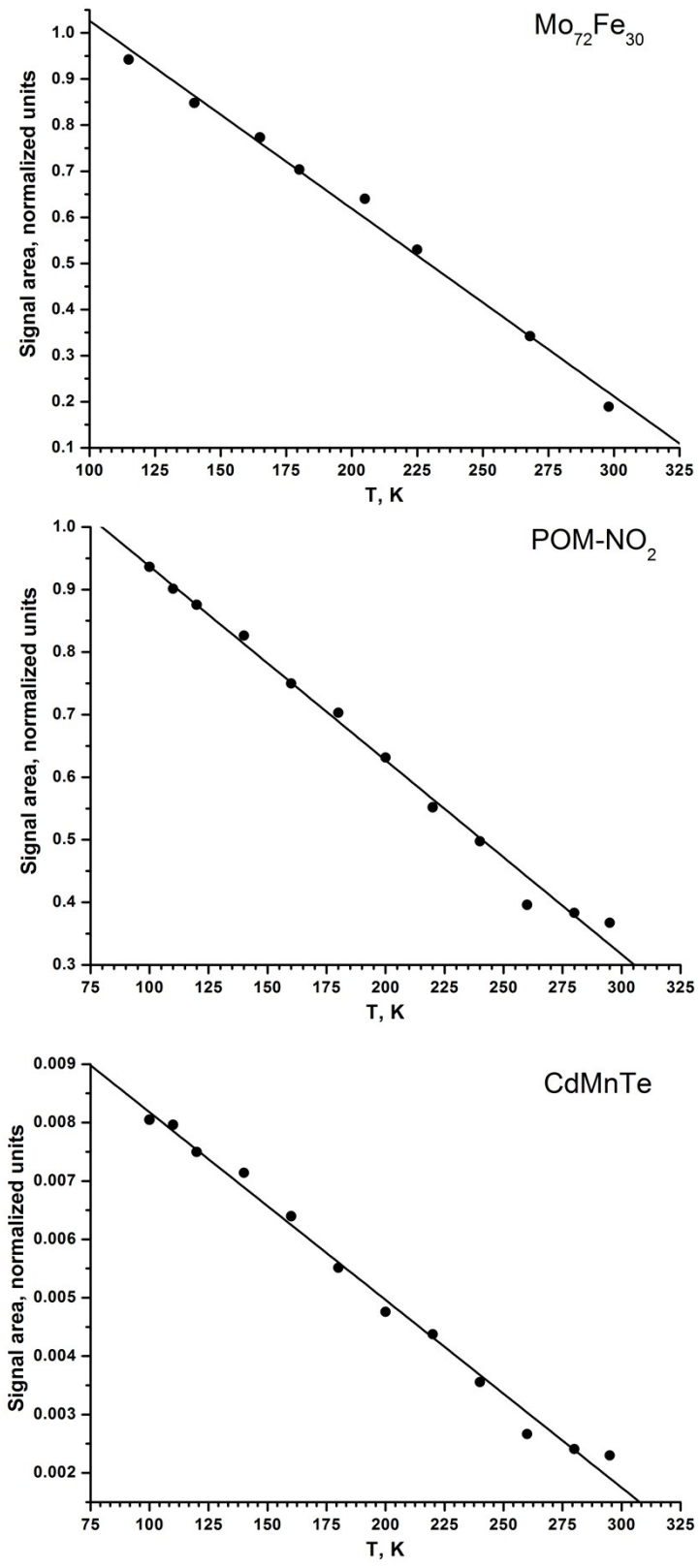

Fig. S8. The comparison of temperature behavior of integral intensity of EPR signals for $Cd_{0.95}Mn_{0.05}Te$, $Mo_{72}Fe_{30}$ and POM-NO_2 samples.

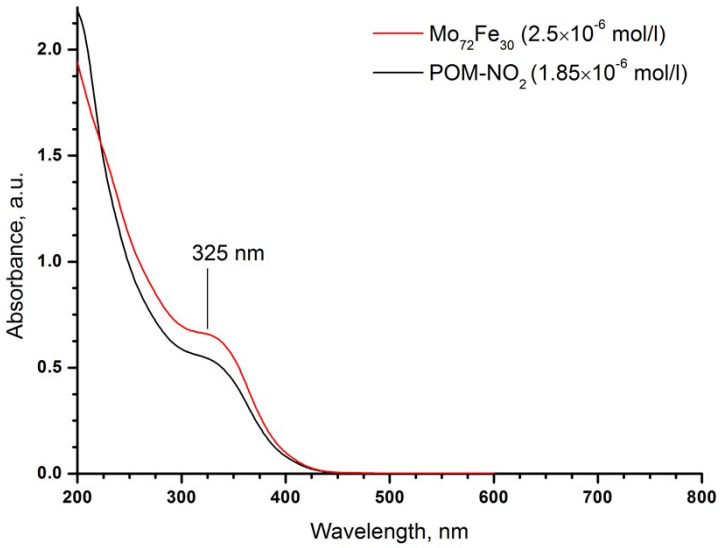

Fig. S9. The comparison of UV-Vis spectra for aqueous solutions of pure $Mo_{72}Fe_{30}$ and POM-NO_2.

References

1 E. Lindholm and G. Sahlström, *Int. J. Mass Spectrom. Ion Phys.*, 1970, **4**, 465–473.

2 B. V. Reddy and S. N. Khanna, *Phys. Rev. Lett.*, 2004, **93**, 068301.

3 H. J. Han, Y. G. Chen, F. M. Yu, J. L. Li, S. Z. Liu and B. H. Wang, *Adv. Mater. Res.*, 2013, **781–784**, 2590–2593.

4 X. Shi, B. Chu, F. Wang, X. Wei, L. Teng, M. Fan, B. Li, L. Dong and L. Dong, *ACS Appl. Mater. Interfaces*, 2018, **10**, 40509–40522.

5 Q. Gao and J. C. Hemminger, *J. Electron Spectros. Relat. Phenomena*, 1990, **54–55**, 667–676.

6 E. C. Housecroft, Catherine E. Constable, *Chemistry: An Integrated Approach*, Addison Wesley Longman, First Edit., 1997.